

PHY180: Pendulum Project

Luyu Wu Vankerkwijk
(Dated: October 22, 2025)

INTRODUCTION

This report investigates the behaviors of a pendulum through experimental analysis, and correlates the findings to the offered closed-form equation of the pendulum:

$$\theta(t) = A_0 e^{-t/\tau} \cos\left(\frac{2\pi t}{T} + \phi_0\right) \quad (1)$$

This equation (Wilson, 2025) gives the angle of the pendulum as a function of time, where A_0 and ϕ_0 are initial conditions, and τ a constant damping factor. T is given as:

$$T = 2\sqrt{L} \quad (2)$$

Experiments were performed using a DIY length-adjustable pendulum and tracked using a camera. Data was processed to determine experimental relationships between amplitude, period, damping, and length.

The period was found to be quadratically related to the angle of oscillation. For $L = 0.75$, where A is the amplitude, and T was fit as $T = aA^2 + bA + c$, values $a = 1.73 \pm 0.0005$, $b = 0.00078 \pm 0.0005$, $c = 0.102 \pm 0.0007$ were found. A small-angle regime where the governing equation is experimentally valid (the quadratic term experimentally disappears) was found to be $A \in [-0.15, 0.15]$. Using the small-angle regime, we investigated the period of the pendulum as a function of length. Equation 2 was verified to be correct within experimental error. This was done through a power fit of the data resulting in $T = [2.00 \pm 0.02]L^{0.51 \pm 0.01}$.

The damping of the system was also investigated as the dimensionless Q-factor ($Q = \pi \frac{\tau}{T}$). Since Q was found to be dependent on amplitude, it was measured at small angles. From lengths varying between $0.15m \rightarrow 0.75m$, the Q-factor was found to roughly align with a negative quadratic fitting term ($-480 \pm 60L^2$) and had a maxima ~ 200 for my setup.

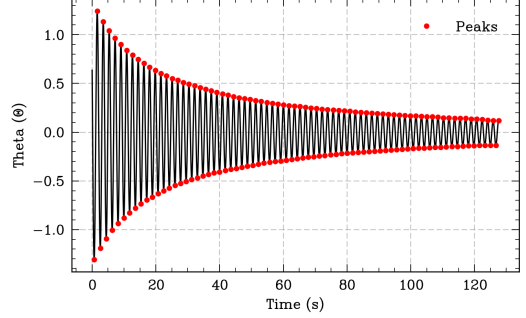


FIG. 1. Plot of pendulum angle against time, along with detected peaks.

EXPERIMENTAL METHODS

The experimental setup consists of a 3m string, wrapped around a cloth hanger attached to an overhang. A cloth hanger is used such that the string can be spooled to adjust the length of the pendulum.

The top of the string is bound tightly. At the bottom of the pendulum, a metal mass with a ring soldered onto it is tied. The mass of the pendulum blob is 54g while the full string's is roughly 2g. A strand length of $74.5cm \pm 0.05cm$ was used in trials where length was kept constant. A calibration ruler is placed on the hanger to provide a reference for tracker.

The pendulum was carefully released by hand. Out-of-plane oscillations were analyzed to ensure minimal effect (see Appendix B).

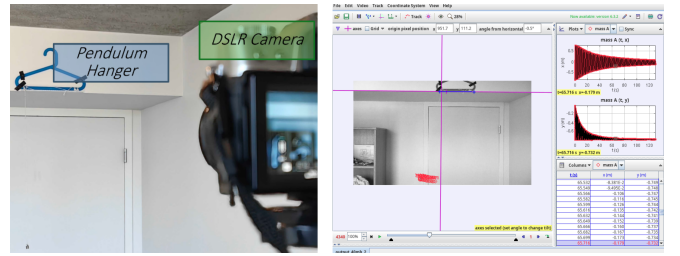


FIG. 2. Picture of experimental setup (Left) and OSP Tracker software (Right). Pendulum blob is visible in the lower left corner. OSP Tracker software used to obtain projected pendulum position as a function of time.

The pendulum system was recorded from approximately 4 meters away (so as to minimize parallax) using a DSLR camera. A shutter speed of $1/1000$ and motion FPS of 60 were used so as to minimize motion blurring, and ensure a high time resolution (roughly 30x the period).

All data was processed in a custom Python script (see

Appendix A). In processing the data, we assume that the motion of the pendulum is continuous (for interpolation between points) so as to achieve better time resolution.

SciPy peak detection was performed to find local maxima. Periods were found by iterating through adjacent peak points and finding the time difference ($T_n = t_{n+1} - t_n$). 'Negative amplitudes' were found with opposite peaks. A visual of this can be seen in Fig. 1.

ANALYSIS

Period Non-Linearity

First, the period non-linearity of the system is analyzed. The governing equation given (eq. 1) assumes the period of the system to be a constant.

By analyzing the relationship between amplitude and period, we can determine if this assumption is correct.

Based on the experimental data plotted in Fig. 3, the period is proportional to A^2 outside 2x the margin of error. Thus it is confident that the period is not constant for this system, and instead varies with amplitude.

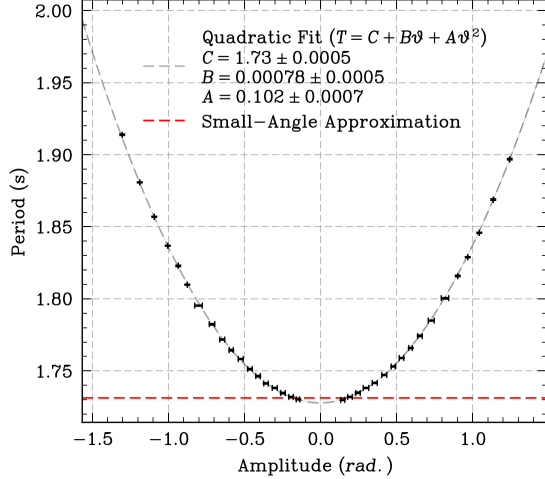


FIG. 3. Plot of pendulum period against oscillation amplitude. Datapoint errorbars are calculated as the standard deviation of the mean. θ as referenced in the legend is the transient amplitude of oscillation. Noticeably, the B is experimentally 0, implying the period is not linearly (asymmetrically) dependent on amplitude.

Subsequent trials are done in amplitude regimes where the change in period is experimentally zero. This correlates to $A \in [-0.15, 0.15]$, where the linear approximation is within error for all values (see Fig. 4).

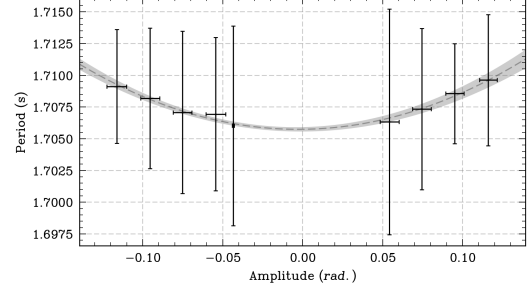


FIG. 4. Plot of pendulum period against oscillation amplitude at small angles. Independent of data shown in Fig. 1, 3.

Damping Factor

Investigating the damping is a critical part of understanding the pendulum's motion. We can define a Q -factor, which defines the ratio of energy loss in relation to a radian of a cycle.

Q -factor can be found using an exponential fit ($Q = \pi \frac{\tau}{T}$). The real pendulum system experiences various damping forces which vary as amplitude decreases. This causes the Q -factor to be non-constant across amplitude in our system as visible in Figure 5. This disagrees with the given equation which gives τ as a constant.

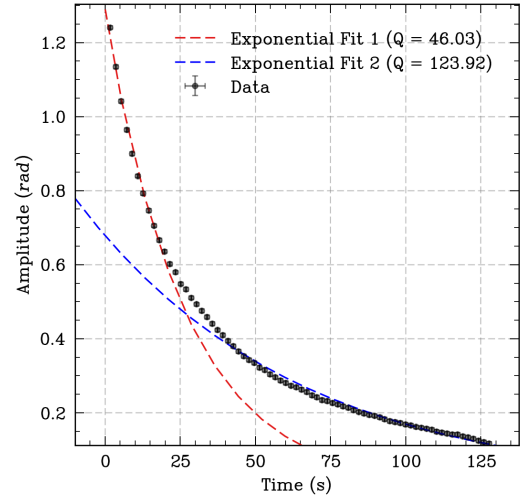


FIG. 5. Plot of pendulum amplitude against time. Two Q -factors are found for different regions where $t_1 \in [0s, 25s]$, $t_2 \in [75s, 125s]$. This shows Q/τ to be amplitude-dependent.

If Q is instead found at low-amplitudes, where the small-angle approximation is more appropriate, we observe a much better fit (Fig. 6).

The Q -factor is found to be 202 ± 0.9 using the fit τ factor. Error is found through the fit error.

Alternatively, the Q -factor can be found by counting the oscillations it takes for the system to dampen to $A_0(e^{-\pi/C})$, then multiplying that number by C (Wilson,

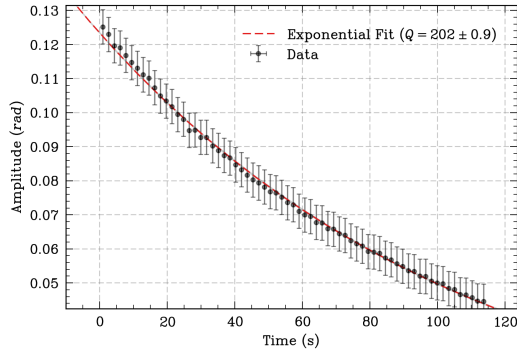


FIG. 6. Plot of pendulum amplitude against time. Since the range of the amplitudes is smaller in this case, an exponential fit is much better.

2025). A visualization of this method can be seen in Fig. 7.

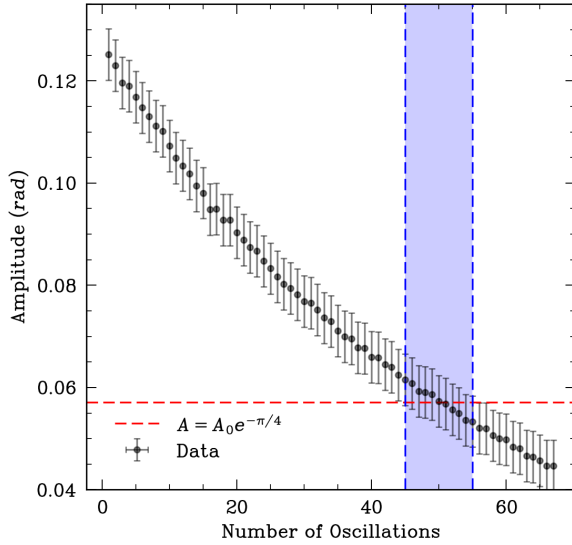


FIG. 7. Amplitude of oscillation vs. oscillation number. Oscillation counting method is used to find number of oscillations before amplitude reaches $e^{-\pi/4}$ (the red line). The blue range represents amplitude peaks which intersect the red line. Here, the number of oscillations is found to be 50 ± 5 , thus Q-factor is found to be 200 ± 20 .

Using oscillation counting, the Q-factor is found to be 200 ± 20 , where the larger error as compared to the exponential fit can be explained by the more discretized methodology.

Importantly, the Q-factors found by the two different methods are highly similar and within error of each other (202 ± 0.9 and 200 ± 20 respectively). This implies an accurate Q-value characterization of the system within the low-amplitude regime.

ADJUSTING LENGTH

Another important part of this lab is investigating the effect of changing the string length of the pendulum.

Length vs. Period

The period as a function of length is given as $T \simeq 2\sqrt{L}$ (Wilson, 2025). Notice the dimensional inconsistency in the equation (stating $s \equiv m^{\frac{1}{2}}$).

To verify this equation, we can collect datapoints from by recording videos using different pendulum lengths (which is easily adjustable as mentioned in Methods).

Each video is composed of at least 100 oscillations, and analyzes a range of oscillations $\theta < 0.15$.

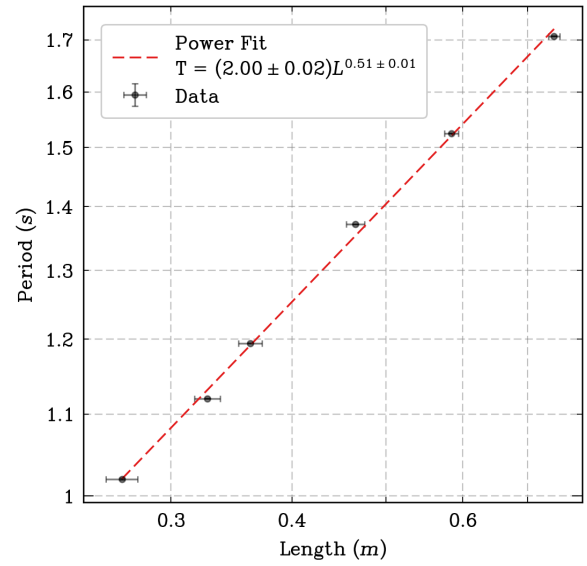


FIG. 8. Log-Log Oscillation Period vs. Length of Pendulum. Each datapoint here represents a distinct tracked movie, where the error is the potential error of the mean.

In Fig. 8, we see that the points, when plotted on a log-log plot form a straight line where $2.00 \ln(L) * 0.51 = \ln(T)$, expanding this, we get $T = 2.00L^{0.51}$, very close to the predicted period, $T = 2\sqrt{L}$.

Length vs. Q-Factor

Next, we investigate the Q-factor of the pendulum in relation to the length. While no prediction is given in Wilson (Wilson 2024), the Q-factor is given as $Q = \frac{\tau}{T}$.

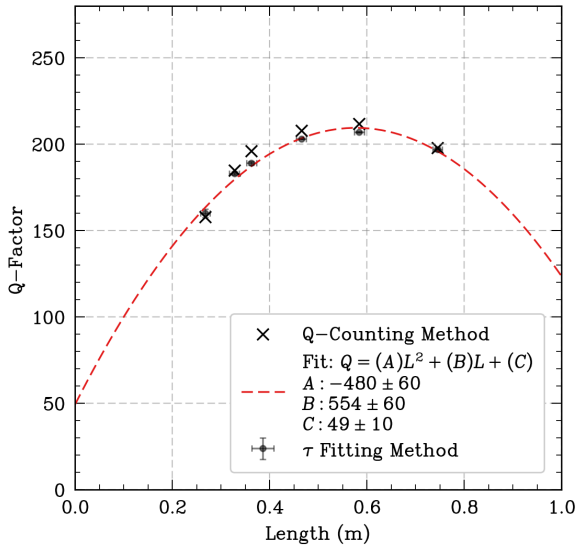


FIG. 9. Q-Factor vs. Length of Pendulum. Each datapoint here represents a distinct tracked movie, where the error is the potential error of the mean.

DETERMINING UNCERTAINTIES

The uncertainty throughout this lab is selected between Type A and Type B depending on which is larger. In this section, the derivation of Type B errors are explained, as they are not immediately clear in certain scenarios, such as when using camera tracking.

The Type B uncertainty of the time of measurement (which propagates to period) is negligible as the camera's shutter speed is 1/1000. Error in period-amplitude plots

is thus calculated through Type A uncertainty. The period error bars likely source from Type-B amplitude uncertainty, which through peak detection (see Appendix C), translates into noise in period measurement.

The uncertainty for the amplitude of the pendulum seen in Figure 6 and 7 are determined through the Type B uncertainty of the amplitude. The width of the pendulum (of which Tracker may not always select the centre of) causes measurement errors. It is calculated as $\epsilon = \frac{w}{2(l)}$ for a 68% confidence. Measurement of the width was done in Tracker to calibrate error to the data (see Appendix C). This error may be minimized by using an indicator (e.g. black dot) instead of tracking the whole blob, however, care must be maintained to avoid rotation of the pendulum around its radial axis.

CONCLUSION

In this report, various aspects of the pendulum's motion were investigated in relation to the offered closed-form equation.

Firstly, a experimental setup consisting of a metal-blob pendulum and DSLR camera was engineered. Precautions were taken to ensure error due to string mass, parallax, and out-of-plane oscillations were minimized.

Secondly, using experimental data, it is proven that T and τ are not constant as the equation suggests, but instead heavily dependent on the amplitude of oscillation (see Fig. 3, 5).

By analyzing oscillations at small angles (within error of a constant period), we are able to characterize the Q-factor of the system (202 ± 0.9). This value was verified using the manual oscillation counting method as well.

APPENDIX

A. Processing Code

All of the code (as well as video files and tracked CSV) used for this project is open-sourced on GitHub, and can be accessed here: <https://github.com/luyu-wu/Pendulum-Project>.

All code is written by me, with credit to modules NumPy, Matplotlib, and SciPy.

B. Out-of-plane Oscillations

In the case that this report investigates, the pendulum has 2 degrees of freedom (ϕ, θ). Since the plane that our camera projects is not sensitive to ϕ , the resultant θ found is dependent on ϕ through $\cos(\phi)x_{\text{pendulum}} = x_{\text{observed}}$.

Thus, tracking the pendulum using a camera, care must be taken to avoid the pendulum going out of plane (in other words, keep ϕ at a desirable constant value).

A solution to this is using purely the y -tracked values, as these are not dependent on ϕ (ignoring parallax, which is not important in our setup). However, at small angles, these are significantly harder to track due to vanishing derivative $\frac{d\cos(\theta)}{d\theta}$ as $\theta \Rightarrow 0$.

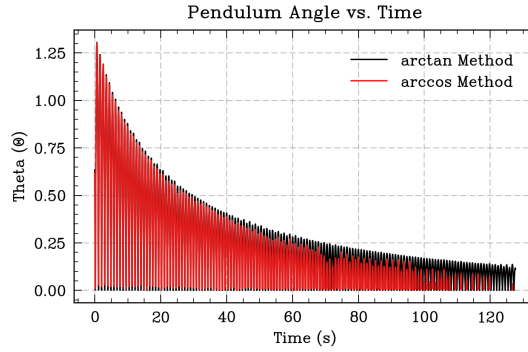


FIG. 10. This graph shows the differences in results between tracking with ϕ dependence and without. Note that the reason no negative θ exists is because that would require us to know ϕ , something not possible purely from y .

C. Measurement Uncertainty of Amplitude

As mentioned in **Determining Uncertainties**, the Type B uncertainty of the pendulum's position must be determined. To find this, the maximum width of the pendulum in the Tracker software is found. This is at the bottom of its motion, where motion blur is greatest. The uncertainty is then found through this via $\epsilon = \frac{w}{2(l)}$ so as to represent a 68% confidence interval. Note that this assumes tracker has a uniform selection density across the pendulum body, which implies this error is overestimated. This process can be seen in Fig. 12.

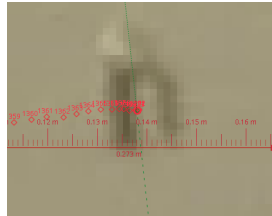


FIG. 11. The measurement of the width of the pendulum is shown here. The length is propagated from the calibration stick.

D: Q-Factor of Different Lengths

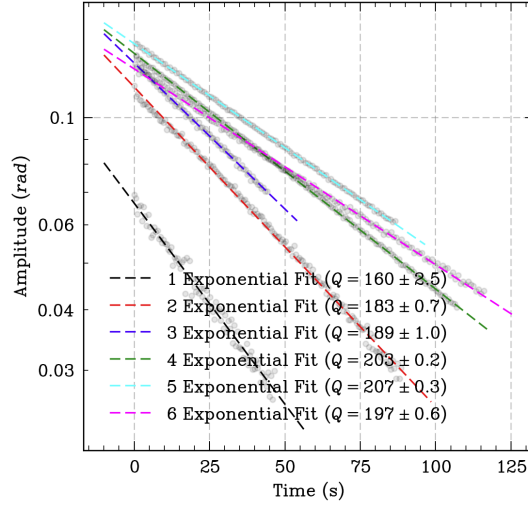


FIG. 12. Here, data from different length trials are plotted together. Note the Y-axis is in log-scale such that the data is linearized.

E: Napkin Math for τ Dependence

Starting with the equation for viscous damping:

$$F_d = -\frac{dr}{dt}c_d \quad (3)$$

Where r is an arbitrary motion vector.

We can write equation of motion with viscous drag in polar coordinates (by solving torque and moment of inertia):

$$\ddot{\theta} = -\sin(\theta)\frac{g}{l} + \dot{\theta}l^2\frac{c_d}{ml^2} \quad (4)$$

We assume c_d to be constant (as it should be a laminar drag dominated effect).

First, taking the small angle approximation, we obtain:

$$\ddot{\theta} = -\theta\frac{g}{l} + \dot{\theta}lc_d \quad (5)$$

Solving the ODE, we obtain:

REFERENCES

Wilson, Brian, “PHY180 Pendulum Project”, from q.utoronto.ca, 2025.

AI Statement

No form of AI was used in planning the lab, writing the lab, or writing the processing code.

AI was used to spell-check the report after finishing with the prompt “Note any typing errors”. 6 minor suggestions regarding spelling mistakes were accepted. I decided to use it because there is no spell checker available in my IDE for LaTeX.